Analytical Solution for Capacitive RF Sheath

MICHAEL A. LIEBERMAN, MEMBER, IEEE

Abstract—**A self-consistent solution for the dynamics of a high voltage, capacitive RF sheath driven by a sinusoidal current source is obtained under the assumptions of time-independent, collisionless ion motion and inertialess electrons. Some results are that 1) the ion sheath thickness s_m is $\sqrt{50/27}$ larger than a Child's law sheath for the same dc voltage and ion current density; 2) the sheath capacitance per unit area for the fundamental voltage harmonic is 1.226 ϵ_0/s_m, where ϵ_0 is the free space permittivity; 3) the ratio of the dc to the peak value of the oscillating voltage is 54/125; 4) the second and third voltage harmonics are, respectively, 12.3 and 4.2 percent of the fundamental; and 5) the conductance per unit area for stochastic heating by the oscillating sheath is 2.98 $(\lambda_D/s_m)^{2/3}(e^2 n_0/mu_e)$, where n_0 is the ion density and λ_D is the Debye length at the plasma-sheath edge, and $u_e = (8eT_e/\pi m)^{1/2}$ is the mean electron speed.**

I. Introduction

LOW-PRESSURE capacitive radio frequency (RF) discharges are widely used for materials processing in the electronics industry. Typical discharge parameters are pressure $p \approx 10$–300 m torr, RF frequency $\omega/2\pi \approx 13.56$ MHz, and RF voltage $V_{RF} \approx 50$–500 V. Almost all the applied voltage is dropped across capacitive RF sheaths at the discharge electrodes. In order to develop adequate models for these discharges, it is important to determine the dynamics and current-voltage characteristics of the sheaths. The sheath dynamics are strongly nonlinear. Only approximate models of the dynamics have appeared in the literature. Godyak and Popov developed a homogeneous model of the sheath [1], [2]. Other authors used a Child–Langmuir law for the ions within the sheath to model the sheath dynamics [3]–[5]. An approximate model of the effect of the time-average electron density on the ion dynamics within the sheath was also developed [6]. The nonlinear ion and electron dynamics are not treated self-consistently within these models. While numerical solutions of the self-consistent dynamics can be obtained [7], they are not particularly illuminating.

In this work we give an analytical, self-consistent solution for the collisionless RF sheath driven by a sinusoidal, RF current source. We obtain expressions for the time-average ion and electron densities, electric field, and potential within the sheath. We also obtain the nonlinear oscillation motion of the electron sheath boundary and the nonlinear oscillating sheath voltage. Finally, we determine the effective sheath capacitance and conductance. The voltages for a single sheath and for a symmetrically driven discharge having two sheaths 180° out of phase are given in a recent report by Godyak [8].

The assumptions of the analysis are as follows:

1) The ion motion within the sheath is collisionless. The ions respond only to the time-average electric field. The ion sheath–plasma boundary is stationary, and ions enter the sheath with a Bohm presheath velocity $u_B = (eT_e/M)^{1/2}$, where e is the ion charge, T_e is the electron temperature (in volts), and M is the ion mass.
2) The electrons are inertialess and respond to the instantaneous electric field. The electron Debye length λ_D everywhere within the sheath is assumed to be much smaller than the ion sheath thickness s_m. This holds provided that $V_{RF} \gg T_e$. Since $\lambda_D \ll s_m$, the electron density falls sharply (within a few Debye lengths) from $n_e \approx n_i$ at the plasma side of the electron sheath boundary to $n_e \approx 0$ at the electrode side. The electron sheath oscillates between a maximum thickness of s_m and a minimum thickness of a few Debye lengths from the electrode surface.

II. Basic Equations

The structure of the RF sheath is shown in Fig. 1. Ions crossing the ion sheath boundary at $x = 0$ accelerate within the sheath and strike the electrode with 50–500 V energies. Since the ion flux $n_i u_i$ is conserved and u_i increases as ions transit the sheath, n_i drops. This is sketched as the heavy, solid line in Fig. 1. The ion particle and energy conservation equations are respectively

$$n_i u_i = n_0 u_B \tag{1}$$

$$\tfrac{1}{2}Mu_i^2 = \tfrac{1}{2}Mu_B^2 - e\bar{\Phi} \tag{2}$$

where n_0 is the plasma density at $x = 0$ and $\bar{\Phi}$ is the time-average potential within the sheath; $\bar{\Phi}$, n_i, and u_i are functions of x. The Maxwell equation for the instantaneous electric field $E(x, t)$ within the sheath is

$$\frac{\partial E}{\partial x} = \frac{e}{\epsilon_0} n_i(x), \qquad s(t) < x$$
$$= 0, \qquad s(t) > x. \tag{3}$$

Here, $s(t)$ is the distance from the ion sheath boundary at $x = 0$ to the electron sheath edge; the electron sheath

Manuscript received February 5, 1988; revised May 3, 1988. This work was supported by the National Science Foundation under Grant ECS-8517363 and by the Department of Energy under Grant DE-FG03-87ER13727.

The author is with the Department of Electrical Engineering and Computer Sciences and the Electronics Research Laboratory, University of California, Berkeley, CA 94720.

IEEE Log Number 8823842.

0093-3813/88/1200-0638$01.00 © 1988 IEEE

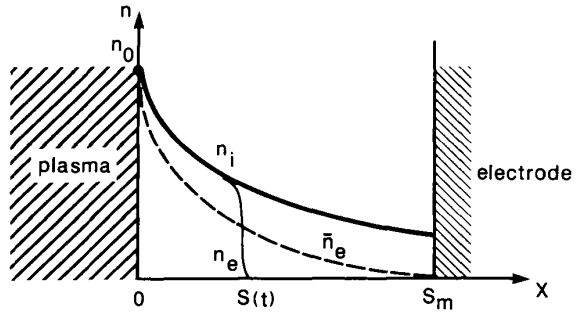

Fig. 1. Structure of the high voltage, capacitive RF sheath.

thickness is $s_m - s(t)$. The instantaneous potential $\Phi(x, t)$ is determined from the equation

$$\frac{\partial \Phi}{\partial x} = -E. \tag{4}$$

Time-averaging (3) and (4) over an RF cycle, we obtain the equations for the time-average electric field $\bar{E}(x)$ and potential $\bar{\Phi}(x)$:

$$\frac{d\bar{E}}{dx} = \frac{e}{\epsilon_0}\left(n_i(x) - \bar{n}_e(x)\right) \tag{5}$$

$$\frac{d\bar{\Phi}}{dx} = -\bar{E} \tag{6}$$

where $\bar{n}_e(x)$ is the time-average electron density within the sheath. We can determine $\bar{E}$, $\bar{\Phi}$, and $\bar{n}_e$ from $s(t)$. For example, we note that $n_e(x, t) = 0$ during the part of the RF cycle when $s(t) < x$; otherwise, $n_e(x, t) = n_i(x)$. We therefore have

$$\bar{n}_e(x) = \left(1 - \frac{2\phi}{2\pi}\right) n_i(x) \tag{7}$$

where $2\phi(x)$ is the phase interval during which $s(t) < x$. Qualitatively, we sketch $\bar{n}_e$ as the dashed line in Fig. 1. For x near zero, $s(t) < x$ during only a small part of the RF cycle; therefore $2\phi \approx 0$ and $\bar{n}_e \approx n_i(x)$. For x near s_m, $s(t) < x$ during most of the RF cycle; therefore $2\phi \approx 2\pi$ and $\bar{n}_e \approx 0$.

To determine the time averages quantitatively, we assume that a sinusoidal RF current density passes through the sheath:

$$J_{RF}(t) = -\tilde{J}_0 \sin \omega t. \tag{8}$$

Equating this displacement current to the conduction current at the electron sheath boundary, we obtain the equation for the electron sheath motion:

$$-en_i(s)\frac{ds}{dt} = -\tilde{J}_0 \sin \omega t. \tag{9}$$

III. Solution

We integrate (3) to obtain

$$E = \frac{e}{\epsilon_0}\int_s^x n_i(\zeta)\, d\zeta, \qquad s(t) < x$$
$$= 0, \qquad s(t) > x. \tag{10}$$

We integrate (9) to obtain

$$\frac{e}{\epsilon_0}\int_0^s n_i(\zeta)\, d\zeta = \frac{\tilde{J}_0}{\epsilon_0 \omega}(1 - \cos \omega t) \tag{11}$$

where we have chosen the integration constant so that $s(t) = 0$ at $\omega t = 0$. From (10) and (11) we obtain

$$E(x, \omega t) = \frac{e}{\epsilon_0}\int_0^x n_i(\zeta)\, d\zeta - \frac{\tilde{J}_0}{\epsilon_0 \omega}(1 - \cos \omega t),$$
$$s(t) < x$$
$$= 0, \qquad s(t) > x. \tag{12}$$

We must time average (12) to obtain $\bar{E}$. Fig. 2 shows a sketch of $s(t)$ versus ωt. We note that $s(t) = x$ for $\omega t = \pm\phi$, and that $s(t) < x$ for $-\phi < \omega t < \phi$. The time average is then

$$\bar{E} = \frac{1}{2\pi}\int_{-\phi}^{\phi} E(x, \omega t)\, d(\omega t). \tag{13}$$

Inserting (12) into (13), we find

$$\bar{E}(x) = \frac{e}{\epsilon_0}\frac{\phi}{\pi}\int_0^x n_i(\zeta)\, d\zeta + \frac{\tilde{J}_0}{\epsilon_0 \omega \pi}(\sin \phi - \phi). \tag{14}$$

Inserting (11) with $s = x$, $\omega t = \phi$ into (14) we obtain

$$\bar{E}(x) = \frac{\tilde{J}_0}{\epsilon_0 \omega \pi}(\sin \phi - \phi \cos \phi). \tag{15}$$

Using (6),

$$\frac{d\bar{\Phi}}{dx} = -\frac{\tilde{J}_0}{\epsilon_0 \omega \pi}(\sin \phi - \phi \cos \phi). \tag{16}$$

Solving (1) and (2) for n_i, we obtain

$$n_i = n_0(1 - 2\bar{\Phi}/T_e)^{-1/2}. \tag{17}$$

Inserting (17) into (9) with $s = x$, $\omega t = \phi$, we obtain

$$\frac{d\phi}{dx} = \frac{(1 - 2\bar{\Phi}/T_e)^{-1/2}}{\tilde{s}_0 \sin \phi} \tag{18}$$

where

$$\tilde{s}_0 = \tilde{J}_0/(e\omega n_0) \tag{19}$$

is an effective oscillation amplitude.

Equations (16) and (18) are the fundamental equations of the self-consistent RF sheath. They are easily solved. Dividing (16) by (18) and integrating, we obtain

$$(1 - 2\bar{\Phi}/T_e)^{1/2} = 1 - H(\tfrac{3}{8}\sin 2\phi - \tfrac{1}{4}\phi \cos 2\phi - \tfrac{1}{2}\phi) \tag{20}$$

where

$$H = \frac{\tilde{J}_0^2}{\pi e \epsilon_0 T_e \omega^2 n_0} = \frac{1}{\pi}\frac{\tilde{s}_0^2}{\lambda_D^2} \tag{21}$$

and $\lambda_D = (\epsilon_0 T_e/en_0)^{1/2}$ is the electron Debye length at $x = 0$. In (20), we have used the boundary condition that

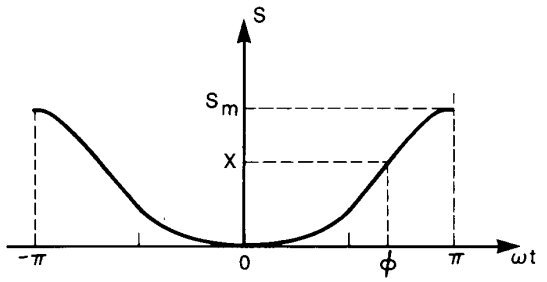

Fig. 2. Sketch of $s(t)$ versus ωt, showing the definition of the phase $\phi(x)$.

$\bar{\Phi} = 0$ at $\phi = 0$ ($x = 0$). Inserting (20) into (18) and integrating again, we obtain

$$\frac{x}{\tilde{s}_0} = (1 - \cos\phi) + \frac{H}{8}\left[\frac{3}{2}\sin\phi + \frac{11}{18}\sin 3\phi - 3\phi\cos\phi - \frac{1}{3}\phi\cos 3\phi\right] \tag{22}$$

where again we have chosen $\phi = 0$ at $x = 0$. Setting $x = s(t)$ and $\phi = \omega t$ in (22), we obtain the nonlinear oscillation motion of the electron sheath, which is shown in Fig. 3 for various values of H. The time-average electric field is given by (15) with $\phi(x)$ obtained from (22). $\bar{E}(x)$ is plotted in Fig. 4. The ion density $n_i(x)$ is found using (17) and (20):

$$\frac{n_i}{n_0} = \left[1 - H\left(\frac{3}{8}\sin 2\phi - \frac{1}{4}\phi\cos 2\phi - \frac{1}{2}\phi\right)\right]^{-1}. \tag{23}$$

This is shown as the solid line in Fig. 5 for $H \gg 1$. Differentiating (15) and using (18) and (20), we obtain the net charge density

$$\frac{\rho}{en_0} = \frac{\phi}{\pi}\frac{n_i}{n_0} \tag{24}$$

and the time-averaging electron density (see also (7))

$$\frac{\bar{n}_e}{n_0} = \left(1 - \frac{\phi}{\pi}\right)\frac{n_i}{n_0}. \tag{25}$$

We give a plot of ρ versus x as the dashed line in Fig. 5. The time-average potential is found from (20)

$$\frac{\bar{\Phi}}{T_e} = \frac{1}{2} - \frac{1}{2}\left[1 - H\left(\frac{3}{8}\sin 2\phi - \frac{1}{4}\phi\cos 2\phi - \frac{1}{2}\phi\right)\right]^2. \tag{26}$$

This is shown in Fig. 6 for $H \gg 1$. For $H \gg 1$, which is the usual case for a capacitive RF discharge, the total dc voltage across the sheath is related to the dc ion current and the ion sheath thickness by an expression that has the form of Child's law:

$$J_i = K\epsilon_0\left(\frac{2e}{M}\right)^{1/2}\frac{\bar{V}^{3/2}}{s_m^2} \tag{27}$$

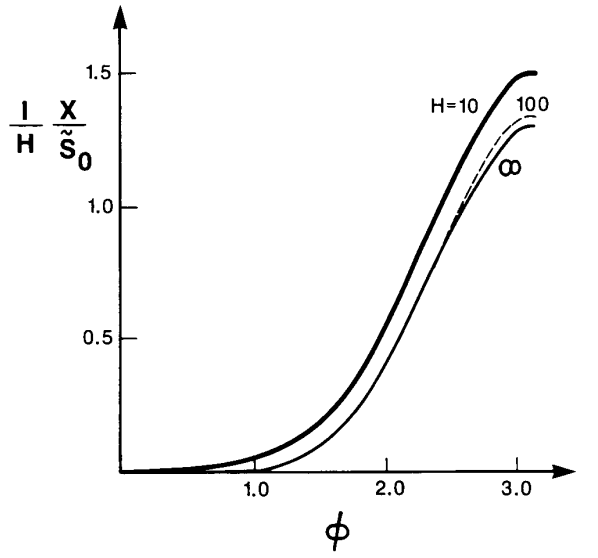

Fig. 3. Normalized position versus phase for the self-consistent RF sheath for various values of the parameter H.

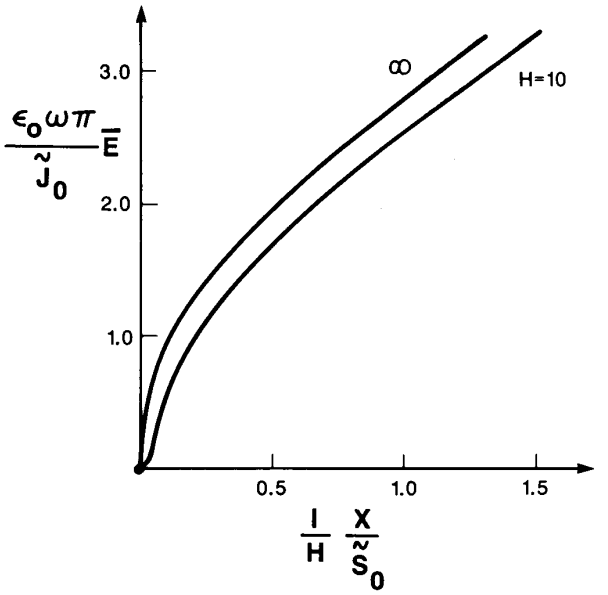

Fig. 4. Normalized electric field versus normalized position for $H = 10$ and $H \gg 1$.

where $J_i = en_0u_B$ is the dc ion current and $\bar{V} = -\bar{\Phi}(\phi = \pi)$ is the voltage across the sheath. From (22) and (26), $s_m/\tilde{s}_0 = 5\pi H/12$ and $\bar{V}/T_e = 9\pi^2H^2/32$. Using (21) for H, we obtain $K = 200/243 \approx 0.82$. In contrast, for Child's law, $K = 4/9 \approx 0.44$. For a fixed current density and sheath voltage, the self-consistent RF ion sheath thickness s_m is larger than the Child's law sheath thickness by the factor $\sqrt{50/27} \approx 1.36$. This increase is produced by the reduction in space charge within the sheath due to the nonzero, time-average electron density.

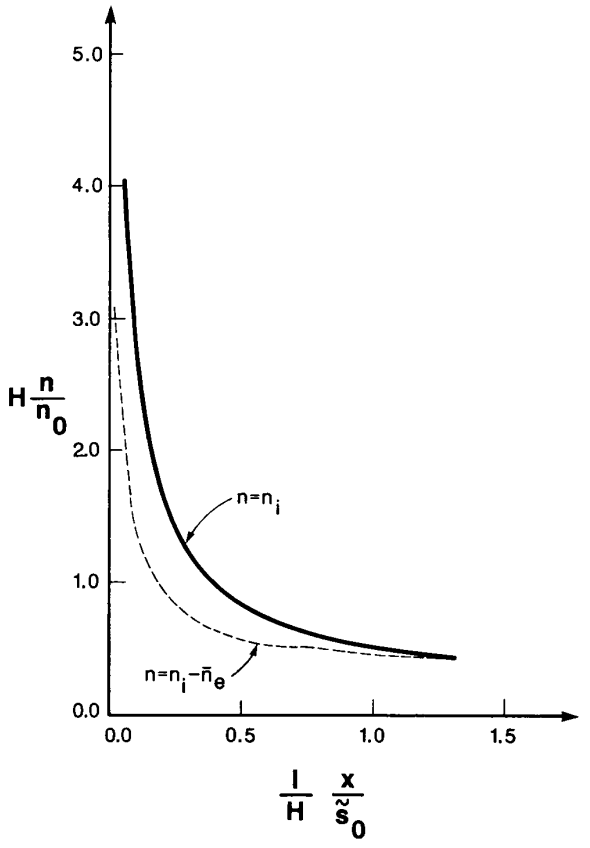

Fig. 5. Normalized ion density n_i and net charge density $n_i - \bar{n}_e$ versus normalized position for $H \gg 1$.

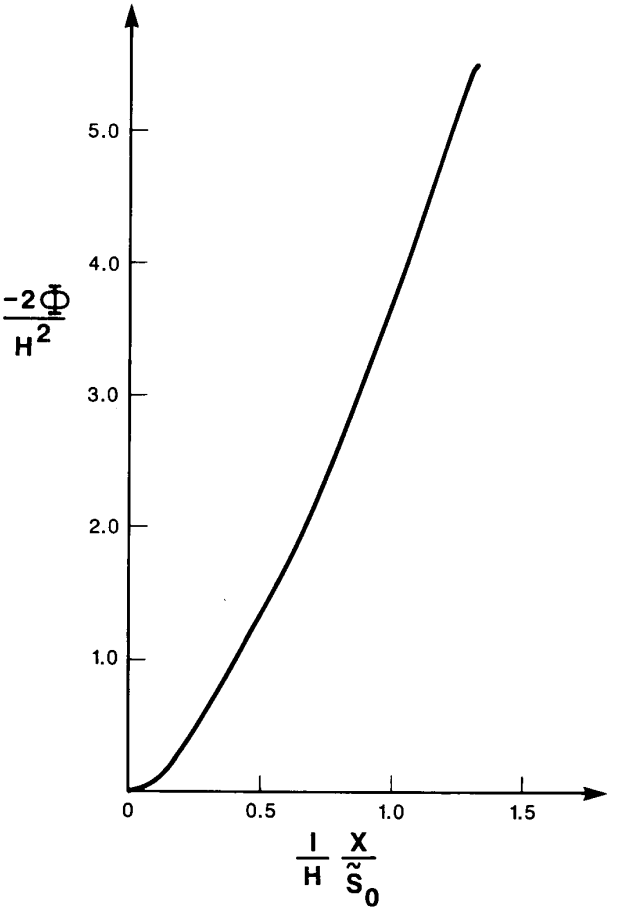

Fig. 6. Normalized time-average potential versus normalized position for $H \gg 1$.

IV. Sheath Capacitance

The instantaneous electric field within the sheath is given by (12). Substituting (11) with $s = x$ and $\omega t = \phi$ into (12), we obtain

$$E(x, t) = \frac{\tilde{J}_0}{\epsilon_0 \omega}(\cos \omega t - \cos \phi), \qquad s(t) < x$$
$$= 0, \qquad s(t) > x. \tag{28}$$

Integrating with respect to x, we obtain the instantaneous voltage from the plasma to the electrode across the sheath

$$V(t) = \int_s^{s_m} E(x, t)\, dx. \tag{29}$$

Changing variables from x to ϕ and using (28), we obtain

$$V(t) = \frac{\tilde{J}_0}{\epsilon_0 \omega} \int_{\omega t}^{\pi} (\cos \omega t - \cos \phi) \frac{dx}{d\phi}\, d\phi. \tag{30}$$

Using (18) and (20) to evaluate $dx/d\phi$ in (30) and integrating, we obtain, for $0 < \omega t < \pi$,

$$V(t) = \frac{\pi H}{4} T_e \Bigg[4 \cos \omega t + \cos 2\omega t + 3 + H\left(\frac{15}{16}\pi + \frac{5}{3}\pi \cos \omega t + \frac{3}{8}\omega t + \frac{1}{3}\omega t \cos 2\omega t + \frac{1}{48}\omega t \cos 4\omega t - \frac{5}{18}\sin 2\omega t - \frac{25}{576}\sin 4\omega t\right)\Bigg]. \tag{31}$$

$V(t)$ is an even, periodic function of ωt with period 2π. For $-\pi < \omega t < 0$, we find that $V(t)$ is given by the right-hand side of (31) with ωt replaced by $-\omega t$. A plot of V versus ωt is given for $H >> 1$ in Fig. 7. The peak value of $V(t)$ occurs at $\omega t = 0$:

$$V(0) = \frac{\pi}{4} HT_e \left[8 + H\left(\frac{125\pi}{48}\right)\right]. \tag{32}$$

Expanding $V(t)$ in a Fourier series

$$V(t) = \sum_{k=0}^{\infty} V_k \cos (k\omega t)$$

we obtain

$$V_0 = \bar{V} = \frac{\pi}{4} HT_e \left[3 + H\frac{9\pi}{8}\right]$$

$$V_1 = \frac{\pi}{2} HT_e \left[2 + H\left(\frac{5\pi}{6} - \frac{1024}{675\pi}\right)\right]$$

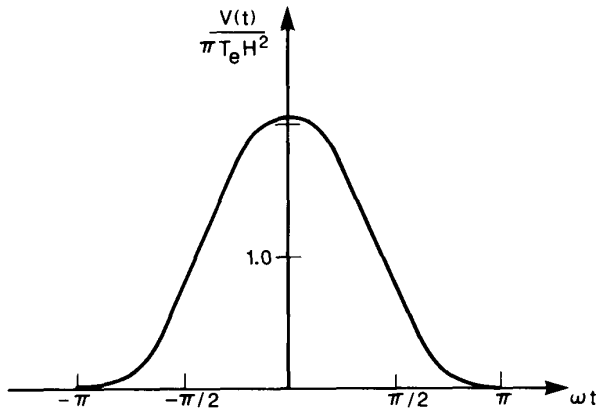

Fig. 7. Normalized time-varying sheath voltage versus ωt for $H \gg 1$.

$$V_2 = \frac{\pi}{2} HT_e\left[\frac{1}{2} + H\frac{\pi}{12}\right]$$

$$V_3 = -\frac{\pi}{2} HT_e\left[H\frac{1024}{3675\pi}\right]. \tag{33}$$

For $H \gg 1$, the second harmonic is 12.3 percent of the fundamental, and the third harmonic is 4.2 percent of the fundamental. The ratio of the dc value to the peak value of the voltage is $\bar{V}/V(0) = 54/125$. Defining the effective capacitance per unit area from the relation

$$-\tilde{J}_0 \sin \omega t = C_s' \frac{d}{dt}(V_1 \cos \omega t)$$

we obtain $C_s' \approx 1.226\ \epsilon_0/s_m$, where $s_m = 5\pi\tilde{s}_0 H/12$ is the ion sheath thickness.

For a symmetrically driven, parallel plate RF discharge (equal-area plates), there are two RF sheaths in series. We let $V_{ap}(t)$ be the voltage on plate a with respect to the plasma and $V_{bp}(t)$ be the voltage on plate b with respect to the plasma. By symmetry, $V_{bp}(\omega t) = V_{ap}(\omega t - \pi)$. The series voltage across both sheaths is $V_{ab} = V_{ap} - V_{bp}$. Using (31), we obtain, for $0 < \omega t < \pi$:

$$V_{ab} = -\frac{\pi}{4} HT_e\left\{8\cos\omega t + H\left[\frac{10}{3}\pi\cos\omega t - \frac{5}{9}\sin 2\omega t - \frac{25}{288}\sin 4\omega t + (2\omega t - \pi)\cdot\left(\frac{3}{8} + \frac{1}{3}\cos 2\omega t + \frac{1}{48}\cos 4\omega t\right)\right]\right\}. \tag{34}$$

The peak-to-peak value of V_{ab} is $2V(0)$, with $V(0)$ given in (32). Expanding V_{ab} in a Fourier series, we obtain

$$V_{ab1} = -\frac{\pi}{4} HT_e\left[8 + H\left(\frac{10\pi}{3} - \frac{4096}{675\pi}\right)\right]$$

$$V_{ab3} = \frac{\pi}{4} HT_e\left[H\frac{4096}{3675\pi}\right]. \tag{35}$$

All even harmonics, including the dc value, are zero, as expected for a symmetrically driven discharge. The third harmonic is 4.15 percent of the fundamental, and the higher harmonics are much smaller. Thus, to a very good approximation, a sinusoidal sheath current leads to a linear response; i.e., a sinusoidal voltage across the discharge. Defining the effective capacitance per unit area of the series combination of the two sheaths from the relation

$$J_{ab}(t) = C'_{\text{sym}} \frac{d}{dt} V_{ab1}(t)$$

we obtain $C'_{\text{sym}} \approx 0.613\ \epsilon_0/s_m$.

V. Sheath Conductance

The RF conductance of the sheath is due to stochastic heating of the electrons by the oscillating sheath. An electron that is reflected from a moving sheath experiences a change of energy. If the sheath moves toward the electron, then the energy increases; if the sheath moves away, then the energy decreases. For an oscillating sheath, some electrons gain energy and others lose energy. However, averaging over an oscillation period, the net effect is an energy gain, corresponding to a *dissipation* in the sheath. This mechanism also has been called "Fermi acceleration" [9]–[12] or "wave riding" [4], [5], [14].

If u is the parallel velocity (along z) of an incident electron at the electron sheath edge $s(t)$ and $u_s(t)$ is the sheath velocity, then the reflected electron has a velocity $u_r = -u + 2u_s$. We let $f_s(u, t)$ be the electron velocity distribution at s, normalized so that

$$\int_{-\infty}^{\infty} f_s(u, t)\, du = n_i(s(t)) = n_s(t).$$

The electron flux Γ_s incident on the sheath is

$$\Gamma_s = \int_0^{\infty} u f_s(u, t)\, du. \tag{36}$$

To determine the power transferred to the electrons, we note that in a time interval dt and for a speed interval du, the number of electrons per unit area that collide with the sheath is given by $(u - u_s) f_s(u, t)\, du\, dt$. This results in a power transfer dS per unit area

$$dS = \tfrac{1}{2} m(u_r^2 - u^2)(u - u_s) f_s(u, t)\, du. \tag{37}$$

Using $u_r = -u + 2u_s$ and integrating overall incident velocities, we obtain

$$S = -2m \int_{u_s}^{\infty} u_s (u - u_s)^2 f_s(u, t)\, du. \tag{38}$$

To determine f_s, we first note that the sheath is oscillating because the electrons in the plasma are oscillating in response to a time-varying electric field. If the velocity distribution function within the plasma in the absence of the electric field is a Maxwellian $g_0(u)$, then the distri-

bution within the plasma is $f_0(u, t) = g_0(u - u_0)$, where $u_0(t)$ is the time-varying oscillation velocity of the plasma electrons. Because $n_s < n_0$, not all electrons having $u > 0$ at $x = 0$ collide with the sheath at s. Many electrons are reflected within the region $0 < x < s$ where the ion density drops from n_0 to n_s. This reflection is produced by a weak electric field whose value is such that $n_e = n_i$ at all times. The transformation of f_0 across this region to obtain f_s is complicated. However, the essential features to determine the stochastic heating are seen if we approximate

$$f_s = \frac{n_s}{n_0} g_0(u - u_0), \qquad u > 0. \tag{39}$$

Inserting (39) into (38) and transforming to a new variable $u' = u - u_0$, we obtain

$$S(t) = -2m \int_{u_s - u_0}^{\infty} u_s n_s \left[u'^2 - 2u'(u_s - u_0) + (u_s - u_0)^2\right] g_0(u')\, du'. \tag{40}$$

Assuming that $|u_s - u_0|$ is much less than the characteristic electron thermal velocity, we can take the lower limit of the integral in (40) to be zero. From (9) we note that

$$n_s u_s = \tilde{u}_0 n_0 \sin\phi \tag{41}$$

and differentiating (22), we obtain

$$u_s - u_0 = \frac{\tilde{u}_0 H}{8}\left[-\frac{3}{2}\cos\phi + 3\phi\sin\phi + \frac{3}{2}\cos 3\phi + \phi\sin 3\phi\right]. \tag{42}$$

Averaging (40) over $\phi = \omega t$ and noting that (41) and (42) are odd functions of ϕ, the first and third terms in (40) average to zero and we obtain

$$\bar{S} = 4m\Gamma_s n_0^{-1} \left\langle (u_s - u_0) u_s n_s \right\rangle_{\phi}. \tag{43}$$

Inserting (41) and (42) into (43) and averaging, we obtain

$$\bar{S} = \frac{3\pi}{32} H m n_0 u_e \tilde{u}_0^2 \tag{44}$$

where for a Maxwellian distribution g_0, the incident flux is

$$\Gamma_s = \frac{1}{4} n_0 u_e \tag{45}$$

and

$$u_e = \left(\frac{8eT_e}{\pi m}\right)^{1/2} \tag{46}$$

is the mean electron speed.

The sheath conductance G_s' per unit area is defined through the relation

$$\bar{S} = \frac{1}{2}\frac{\tilde{J}_0^2}{G_s'} \tag{47}$$

where $\tilde{J}_0 = en_0\tilde{u}_0$. Equating (44) and (47), we obtain

$$G_s' = \frac{16}{3\pi H}\left[\frac{e^2 n_0}{m u_e}\right]. \tag{48}$$

We note, using (21) and the definition of s_m, that

$$H = \left[\frac{144}{25\pi^3}\right]^{1/3}\left[\frac{s_m}{\lambda_D}\right]^{2/3}. \tag{49}$$

We then obtain

$$G_s' = 2.98\,\frac{e^2 n_0}{m u_e}\left[\frac{\lambda_D}{s_m}\right]^{2/3}. \tag{50}$$

This effective surface conductance per unit area represents a powerful electron heating mechanism in a capacitive RF discharge.

As an example for a plasma processing discharge, we choose $\bar{V} = 200$ V, $T_e = 3$ eV, $J_i = 0.5$ mA/cm^2, $\omega = 2\pi \times 13.56$ MHz, and $M = 69$ amu (i.e., CF_3^+). Then we obtain $u_B = 2.04 \times 10^5$ cm/s, $n_0 = 1.53 \times 10^{10}$ cm^{-3}, $H = 4.9$, $\tilde{J}_0 = 8.52$ mA/cm^2, $\tilde{s}_0 = 4.08 \times 10^{-2}$ cm, $\lambda_D = 1.04 \times 10^{-2}$ cm, $s_m = 0.262$ cm, $C_s' = 0.414$ pF/cm^2, $\tilde{u}_0 = 3.48 \times 10^6$ cm/s, $u_e = 1.16 \times 10^8$ cm/s, $\bar{S} = 2.83 \times 10^{-3}$ W/cm^2, and $G_s' = 1.29 \times 10^{-2}$ S/cm^2. The dc ion power flux incident on the electrode is $S_i = J_i \bar{V} = 0.1$ W/cm^2.

For a homogeneous (uniform ion density) sheath, $n_s = n_0$ and $u_s = u_0$. Then the integral in (40) vanishes and there is no stochastic heating: $G_s' \to \infty$. We can understand this physically as follows: In the accelerated frame moving with the plasma, the electron sheath edge at $s(t)$ is stationary; therefore, no energy is transfered to electrons that collide with the sheath. Preliminary results from a self-consistent computer simulation verify this conclusion [15]. Thus the nonhomogeneous nature of the self-consistent ion density within the RF sheath is an essential feature of the stochastic heating mechanism.

Acknowledgment

Helpful discussions with W. S. Lawson, A. J. Lichtenberg, G. Misium, and S. Savas are gratefully acknowledged.

References

[1] V. A. Godyak, *Sov. J. Plasma Phys.*, vol. 2, p. 78, 1976.
[2] V. A. Godyak and O. A. Popov, *Sov. J. Plasma Phys.*, vol. 5, p. 227, 1979.
[3] H. R. Koenig and L. I. Maissel, *IBM J. Res. Develop.*, vol. 14, p. 168, 1970.
[4] J. M. Keller and W. B. Pennebaker, *IBM J. Res. Develop.*, vol. 23, p. 3, 1979.

[5] W. B. Pennebaker, *IBM J. Res. Develop.*, vol. 23, p. 16, 1979.
[6] V. A. Godyak and Z. K. Ganna, *Sov. J. Plasma Phys.*, vol. 6, p. 372, 1980.
[7] V. A. Godyak and S. N. Oks, *J. Phys.* (Paris), vol. 40, p. C7-809, 1979.
[8] V. A. Godyak, *Soviet Radio Frequency Discharge Research.* Falls Church, VA: Delphic Assoc., 1986, pp. 110-113.
[9] E. Fermi, *Phys. Rev.*, vol. 75, p. 1169, 1949.
[10] V. A. Godyak, *Sov. Phys.—Tech. Phys.*, vol. 16, p. 1073, 1972.
[11] A. I. Akiezer and Z. K. Bakai, *Sov. Phys. Dokl.*, vol. 16, p. 1065, 1971.
[12] A. J. Lichtenberg and M. A. Lieberman, *Regular and Stochastic Motion.* New York: Springer-Verlag, 1983, sec. 3.4.
[13] O. A. Popov and V. A. Godyak, *J. Appl. Phys.*, vol. 57, p. 53, 1985.
[14] M. J. Kushner, *IEEE Trans. Plasma Sci.*, vol. PS-14, p. 188, 1986.
[15] W. S. Lawson, M. A. Lieberman, and C. K. Birdsall, "Electron dynamics of RF driven parallel plate reactor" presented at the IEEE Int. Conf. on Plasma Sci. (Seattle, WA), June 1988.